

UC Davis

UC Davis Previously Published Works

Title

Label-Free Assessment of Collagenase Digestion on Bovine Pericardium Properties by Fluorescence Lifetime Imaging

Permalink

<https://escholarship.org/uc/item/5hf0h7tv>

Journal

Annals of Biomedical Engineering, 46(11)

ISSN

0145-3068

Authors

Li, Cai
Shklover, Jeny
Parvizi, Mojtaba
[et al.](#)

Publication Date

2018-11-01

DOI

10.1007/s10439-018-2087-6

Peer reviewed



Published in final edited form as:

Ann Biomed Eng. 2018 November ; 46(11): 1870–1881. doi:10.1007/s10439-018-2087-6.

Label-Free Assessment of Collagenase Digestion on Bovine Pericardium Properties by Fluorescence Lifetime Imaging

Cai Li¹, Jeny Shklover², Mojtaba Parvizi³, Benjamin E. Sherlock², Alba Alfonso Garcia², Anne K. Haudenschild², Leigh G. Griffiths³, Laura Marcu^{2,4}

¹Department of Materials Science Engineering, University of California, Davis, Davis, CA, USA

²Department of Biomedical Engineering, University of California, Davis, Davis, CA, USA

³Department of Cardiovascular Medicine, Mayo Clinic, Rochester, MN, USA

⁴Department of Biomedical Engineering, University of California, Davis, 2513 GBSF, Davis, CA 95616, USA

Abstract

The extracellular matrix architecture of bovine pericardium (BP) has distinct biochemical and biomechanical properties that make it a useful biomaterial in the field of regenerative medicine. Collagen represents the dominant structural protein of BP and is therefore intimately associated with the properties of this biomaterial. Enzymatic degradation of collagen molecules is critical for extracellular matrix turnover, remodeling and ultimately tissue regeneration. We present a quantitative, label-free and non-destructive method for monitoring changes in biochemical and biomechanical properties of BP during tissue degradation, based on multi-spectral fluorescence lifetime imaging (ms-FLIm). Strong correlations of fluorescence intensity ratio and average fluorescence lifetime were identified with collagen content, Young's Modulus and Ultimate tensile strength during collagenase degradation, indicating the potential of optically monitoring collagen degradation using ms-FLIm. The obtained results demonstrate the value of ms-FLIm to assess the quality of biomaterials *in situ* for applications in regenerative medicine.

Keywords

Fluorescence lifetime imaging; Collagenase degradation; Non-destructive monitoring

INTRODUCTION

Extracellular matrix (ECM) is a complex, 3D environment that plays a key role in determining the structure and function of tissues and organs. Pericardium is a clinically utilized biomaterial with distinct biochemical and biomechanical properties.¹⁵ In particular,

Address correspondence to Laura Marcu, Department of Biomedical Engineering, University of California, Davis, 2513 GBSF, Davis, CA 95616, USA. lmarcu@ucdavis.edu.

ELECTRONIC SUPPLEMENTARY MATERIAL

The online version of this article (<https://doi.org/10.1007/s10439-018-2087-6>) contains supplementary material, which is available to authorized users.

bovine pericardium (BP) is an attractive candidate biomaterial for regenerative medicine because of its composition, collagen architecture, and homogeneity. Current clinical applications of glutaraldehyde-fixed bovine pericardium include vascular,²¹ cardiac,³² thoracic²⁴ and urologic surgeries,³³ as well as ophthalmologic applications.¹³ However, while glutaraldehyde-fixation can mask BP from recipient graft-specific immune responses, this treatment also renders the biomaterial incompatible with normal ECM repair and replacement processes.²⁸ Regenerative medicine approaches aim to remove components that stimulate recipient immune responses, while retaining native ECM structure and function properties.¹⁰ Since type I collagen represents the predominant structural protein of BP, accounting for approximately 70% of the biomaterial dry weight (DW), assessment of collagen quality is critical for the development and application of BP based biomaterials.³⁵ The mechanical properties of such biomaterials are also critical in determining their long term function.^{3,5} *In vitro* collagen degradation by collagenase digestion is a widely used method to characterize the quality in terms of collagen content and matrix mechanics of this and other collagen rich biomaterials.^{12,29} During degradation, hydroxyproline assay can be utilized to measure loss of collagen in pericardium while mechanical properties can be measured by several mechanical tests (i.e., uniaxial tensile testing, biaxial tensile testing, compressive testing or cyclic loading).¹ However, such conventional analyses of both collagen content and mechanical properties are costly, time consuming and result in sample destruction, rendering them incompatible with assessments of individual samples prior to *in vivo* implantation.

Label-free optical imaging techniques provide non-destructive methods to characterize biomaterial degradation by quantitatively monitoring their collagen content and mechanical properties. For example, optical coherence tomography (OCT) has been widely used for cross-sectional imaging of tissue anatomy with micrometer resolution. Studies showed that one of its sub-modalities, polarization-sensitive OCT, is capable of quantifying collagen content by measuring the tissue birefringence.²² In addition, optical coherence elastography (OCE), is capable of quantitatively measuring tissue mechanical properties.³⁰ However, an independent loading system is required for performing OCE measurement, which increases the cost and complexity of this approach. A recent study demonstrated the possibility of utilizing second harmonic generation (SHG) signal and two photon excitation fluorescence (TPEF) to predict the compositional and mechanical changes of ECM after myocardial infarction.²⁵ The study showed that the SHG and TPEF signals were correlated with the collagen content and elastic moduli of the ECM. Although the longer excitation wavelengths used in SHG and TPEF and the non-linear dependence of absorption as a function of intensity allows for deeper penetration and 3D sectioning capabilities, the cost and complexity of fiber-based multiphoton imaging mean that it is not well suited to widespread use as a tool for evaluating engineered tissue *in vitro*.

Collagen is an endogenous fluorophore with high quantum efficiency. Thus, measuring autofluorescence (AF) under UV excitation is a powerful method for monitoring the properties of collagen based biomaterials.¹⁴ Single photon AF of endogenous fluorophores in the ECM can be used to directly determine the morphofunctional properties of biomaterials.⁴ Lewis *et al.* demonstrated a correlation between endogenous AF measured with a spectrofluorometer and biomechanical stiffness in bovine articular cartilage, and suggested using the

endogeneous UV fluorescence intensity as a bio-marker for monitoring the functional state of cartilage.¹⁴ Alternatively, narrow spectral excitation and collection bands can be selected for fluorescence imaging. In addition, fluorescence lifetime (FL), a measure of the average time a fluorophore takes to return to its electronic ground state following excitation to a higher energy state, has also been shown to distinguish different molecular species. Similar to fluorescence spectrum, FL is intrinsically related to the tissue composition but is independent of fluorophore concentration, the excitation efficiency and the emission detection geometry. Studies have shown that fluorescence lifetime imaging (FLIm) is a powerful optical tool for label-free monitoring of the state of biological tissues like porcine articular cartilage and cardiovascular tissues.^{19,20} Moreover, FL is highly sensitive to the fluorophore microenvironment that is associated with the molecular structure of tissues¹⁸ and may provide another approach to characterize tissue structure during the degradation process of BP. In addition, compared with the modalities described above, AF measurement has the advantage of directly assessing tissues bio-chemical composition. Also, AF can be easily used *in vivo* and *in vitro* study because of the convenience brought by guiding light through fiber optics

The multi-spectral fluorescence lifetime imaging (ms-FLIm) system developed in our laboratory is capable of simultaneously detecting the changes in spectral emission and fluorescence lifetime of unlabeled tissue samples in distinct wavelength bands.³⁶ In this work, we use ms-FLIm to non-destructively assess changes in the composition and mechanical properties of native BP following partial digestion of the matrix using bacterial collagenase. We compared FLIm measurements with the results of hydroxyproline assays, for collagen content, and tensile testing, for Young's Modulus and Ultimate tensile strength (UTS) estimation, at different levels of collagenase digestion. The ms-FLIm system's sensitivity was calibrated by performing pair-wise correlation analysis between the fluorescence parameters and conventional measurement results. In addition, we studied the effect of solvent polarity to explain the observed changes of emission spectrum and lifetime. Finally, we demonstrated the system's non-destructive imaging capability by measuring a localized digestion of BP.

MATERIALS AND METHODS

BP from young adult cattle were ordered from Spear Products, Coopersburg, PA. Following removal of connective tissue and pericardial fat, the tissue was trimmed and cut into stripes that were frozen in Dulbecco's Modified Eagle Medium (DMEM) with 15% (v/v) dimethyl sulfoxide (DMSO) at - 80 °C. Samples used in the experiment were thawed, then washed in phosphate-buffered saline (PBS), pH 7.4, for 30 min, and finally cut to small round discs using 5 mm biopsy punches. For consistency, the control and digested groups went through the same procedure and all the samples were harvested from the same batch.

Samples were divided into two groups: control and digested. Control samples were placed in 2 ml Hank's Balanced Salt Solution (HBSS), and digested samples were placed in 2 ml 200 U ml⁻¹ Clostridium histolyticum collagenase type I (Gibco, Carlsbad, CA) diluted by HBSS. Samples were incubated at 37 °C for 0, 8, 16 or 24 h, and then washed at room temperature with phosphate buffered saline (PBS). The digestion exposure time of samples

for tensile test (0, 8, 12 h) were different from the ones used in other tests because the samples after 16 h became too soft to be transported to the measuring stage without any damage. In order to remove the residual collagenase and fiber debris before measuring, all the samples were rinsed in PBS for 5 min, then washed with fresh PBS on a shaker for 24 h, and rinsed with fresh PBS again for 5 min. After washing, samples were subjected to tensile testing, hydroxyproline assay, and histology. Samples tested for tension and collagen content were previously imaged with the ms-FLIm system. All digestion experiments were conducted with $N=6$ per group per time point.”

The ms-FLIm system is based on a previously reported principle.³⁶ Excitation was performed by a 355 nm UV laser (STV-02E, TEEM photonics, France), the light from which is guided to the sample using a 2 m long, 400 μm core flexible multimode optical fiber (Polymicro Technologies, Phoenix, AZ). Sample fluorescence is collected using the same fiber optic. A custom wavelength selection module is used to divide the autofluorescence into three distinct spectral bands (Channel 1: 390/18 nm, Channel 2: 435/40 nm; Channel 3: 510/84 nm). Each spectral band has its own fiber optic delay line, used to temporally multiplex the light from the three spectral bands onto a single microchannel plate photomultiplier tube (MCP PMT) detector. The fluorescence dynamics are recorded using a high speed digitizer operating at 12.5 GS/s (PXIe-5185, National Instruments, Austin, TX). Fluorescence intensity is calculated by integrating the recorded fluorescence decay. Intensity ratios of each spectral channel are obtained by dividing that channel’s intensity over the sum of all channels’ intensities. The average fluorescence lifetime is calculated as the expectation value of the probability density function of the decay. The temporal instrument response function is deconvolved from the raw fluorescence decay using a constrained least-squares deconvolution with Laguerre expansion.¹⁶ The spatial distribution of fluorescence intensity and lifetime is measured by raster scanning the fiber optic distal tip across the sample surface using a 3-axis translation stage (MT S50-Z8, Thorlabs, Newton, NJ).

Collagen content of BP samples was determined as previously described ($N=6$ samples per time point).³⁴ Samples were weighed [wet-weight (WW)], lyophilized for 72 h and weighed again (DW). Lyophilized samples were digested in 5N HCl (1 ml per 10 mg DW) at 120 °C for 24 h. Bovine collagen type I (Chondrex Inc., Redmond, WA) was digested similarly and served as a reference. Sample collagen content per DW was quantified using collagen I standards and a Hydroxyproline Assay Kit (Chondrex Inc., Redmond, WA).

Tensile testing was conducted using a uniaxial materials testing machine (Test Resources, Shakopee, MN), as previously described.³⁴ After ms-FLIm measurements, BP samples were cut into dog-bone shaped tensile specimens parallel to the primary collagen fiber direction. Sample thickness and width were measured *via* ImageJ software (NIH, Bethesda, MD).²⁶ A uniaxial strain to failure test was conducted with a fixed gauge length of 1.5 mm and a strain rate of 1% of the gauge length per second. For each sample, load-displacement curves were normalized to specimen cross-sectional area. The apparent Young’s Modulus was calculated by least squares fitting the linear portion of the resulting stress-strain curve in Matlab v2018a (Mathworks Inc., Natick, MA) while the UTS was defined at the maximum stress.

Formalin-fixed, paraffin-embedded 5 mm biopsy punches of control and digested samples ($N=6$ per group per time point) were histologically processed for hematoxylin and eosin (H&E), and PicroSirius Red (PSR) stainings, according to standard procedures. Images were captured using Aperio ScanScop and processed using ImageScope software 12.3.2.5030 (Leica Microsystems Inc., IL, USA). H&E staining was used to assess general tissue morphology, and PSR staining was used to specifically visualize collagen fiber structures..

For explaining the observed changes of emission spectrum and lifetime, the effect of solvent was studied by measuring native and 16 h digested BPs in solutions of different polarities. The solutions were made by mixing PBS with pure (100%) ethanol at different volume ratios. Since ethanol is less polar than water, increasing the solvent ethanol concentration decreases the polarity of the solvent. Four 16 h digested samples (processed the same as described above) were measured by ms-FLIm in the pure PBS, 30% ethanol, 60% ethanol and pure ethanol, while the remaining two native BP samples were measured in pure PBS and pure ethanol for comparison. The measurements were taken immediately after samples were immersed in ethanol solutions to avoid collagen structure being changed.³¹

To demonstrate the ms-FLIm system's capability of performing non-destructive measurement, we created samples with heterogeneous distributions of collagen content by digesting native BP at specific locations. As shown later in "Results" section, BP pieces (1 cm \times 1 cm) were immersed in 3 ml HBSS. Three cylinders (Pyrex® cloning cylinder O.D. \times H 6 mm \times 8 mm) were placed on top of BP: one cylinder (control) was filled in with 70 μ l HBSS, and the other two (digested) contained 200 U ml⁻¹ collagenase for one or two days. A small metal rod placed on the cover of a well plate was used to gently press the cylinders against BP in order to avoid solution leaking out their base. Before optical measurements, samples were rinsed with PBS for 5 min, then washed with fresh PBS for 24 h, and finally rinsed with fresh PBS for another 5 min.

Kruskal Wallis H test was performed to compare the mean intensity ratios and fluorescence lifetimes of all the control and digested groups. The difference between the control and digested groups were analyzed using Mann-Whitney U test and quantified by calculating the unstandardized mean difference. The Kendall τ_B correlation analysis³⁷ was performed for analyzing the ordinal correlation between ms-FLIm results (intensity ratio, lifetime) and conventional measurement results (collagen content, Young's modulus, UTS). A predictive analysis using multi-variable linear regression (MLR) is attempted and shown in supplementary materials in order to estimate the predicting ability of ms-FLIm. The statistical analysis was performed using MATLAB 2016a and RStudio.

RESULTS

The effect of collagenase degradation is shown in Fig. 1. H&E staining was used as the gold standard for imaging tissue morphology and demonstrated that collagenase treatment resulted in the degradation of ECM components. Fewer fiber structures remained were observed in the tissue samples after longer digestion times (Fig. 1a). In terms of collagen density, PSR staining, which specifically stains collagen in red, showed that after 8 h digestion, wavy collagen fibers were still present; however, the distance between fibers

became much larger and fibers were noticeably thinner than in native tissue. Following 16 h digestion the fibers started to disassemble into fibrils. After 24 h, collagen disruption was more severe and only small wavy fiber were observed with markedly disrupted organization (Fig. 1b). The lightening of PSR staining image also indicates the decrease of collagen content during collagenase degradation.

Quantitative analysis of collagen content was performed using hydroxyproline assay. As shown in Fig. 1c, collagen content of the digested group decreased dramatically over the timecourse of collagen degradation ($63.14 \pm 1.87\%$ reduction in collagen content per DW after 24 h), while the control group remained constant. The decrease of collagen content for the digested group compared to the control group is shown to be associated with digestion exposure time. The value of collagen content are also included in the supplementary material Table. S1.

Since collagen is the dominant ECM structural protein in BP, collagen degradation and removal results in a considerable change of the biomaterial mechanical properties. As demonstrated by tensile testing, the digested group became softer after collagenase degradation. Both of Young's Modulus and UTS of the digested group became smaller with digestion exposure time, while the control group did not show significant variation (Table 1).

Intensity ratio and fluorescence lifetime maps recorded in Channel 1 (390/18 nm) for the digested group at different time points are shown in Fig. 2. As mentioned in "Materials and Methods", the intensity ratio is defined as an indicator of fluorescence spectra. Both fluorescence spectra and fluorescence lifetime can be used for analyzing the compositional changes in BP. A clear continuous decrease is found for both the intensity ratio and fluorescence lifetime in Channel 1. Given the homogeneity of the sample, a circular region of interest (ROI) for each sample was manually selected (black circles in Fig. 2) and data in each channel within the ROI were analyzed. Channel 3 (510/84 nm) will not be discussed further because very low correlation was found with the conventional measurement results.

The statistical analyses were done for 6 control and 6 digested groups at digestion exposure time 0, 8, 16 and 24 h. Figures 3 and 4 show the changes of intensity ratio and fluorescence lifetime, respectively. Kruskal Wallis H test results show a statistically significant difference between the digested groups over different exposure times ($p < 0.05$), but no difference for the control groups ($p > 0.05$). The Mann-Whitney U test shows that Channel 1 (390/18 nm) and Channel 2 (435/40 nm) intensity ratios of the digested group are statistically different from those of the control group after collagenase degradation ($p < 0.05$; Figs. 3a and 3b). Channel 1 intensity ratio decreased 0.26 ± 0.02 after 24 h of collagenase degradation, whereas Channel 2 intensity ratio increased 0.14 ± 0.01 after 24 h, indicating that the fluorescence spectra of BP red shifted after collagenase degradation. This spectral red-shift is quantitatively demonstrated by the change of intensity ratio using unstandardized mean difference between the control and digested groups, which shows a clear increasing trend in absolute values with digestion exposure time (Figs. 3a and 3b).

The trend of change agrees with the hydroxyproline assay results (Fig. 1d), where the collagen content difference between 16 and 24 h is smaller than that between 8 and 16 h.

The same statistical analysis was performed for Channel 1 (390/18 nm) and Channel 2 (435/40 nm) fluorescence lifetime (Fig. 4). A decrease of fluorescence lifetime is observed for both Channel 1 and Channel 2 for later time points of collagenase digestion. However, the decrease of fluorescence lifetime was not significant at early stages of collagenase digestion before 16 h time point. For Channel 1, there were significant decreases of 0.36 ± 0.10 ns on average after 16 h digestion, and 1.37 ± 0.12 ns on average after 24 h (Figs. 4a and 4c). For Channel 2, there was no significant change till the last time point when we found an average of 1.07 ± 0.13 ns decrease (Figs. 4a and 4b).

Kendall τ_B correlation analysis shows that different metrics of ms-FLIm data were correlated with the collagen content, Young's Modulus and UTS (Figs. 5 and 6). Intensity ratios in Channel 1 (390/18 nm) and Channel 2 (435/40 nm) were significantly correlated with collagen content, Young's Modulus and UTS ($p < 0.01$, Fig. 5). Fluorescence lifetime in Channel 1 correlated with the collagen content ($p < 0.01$, Fig. 6a), while the lifetime in Channel 2 did not ($p = 0.47$, Fig. 6d). Both of Channel 1 and Channel 2 lifetime showed correlations with Young's Modulus and UTS ($p < 0.01$, Fig. 6).

The effect of solvent polarity on fluorescence lifetime and intensity ratio is shown in Fig. 7. The polarity of solvent increases when ethanol is mixed with PBS in less concentration. As shown in Figs. 7a and 7b, for 16 h digested BP, with increasing solvent polarity, Channel 1 (390/18 nm) intensity ratio decreased and Channel 2 (435/40 nm) intensity ratio increased. This is consistent with the red shift we observed after collagenase degradation (Fig. 3). For native BP, a red shift also occurred for samples measured in ethanol, but the observed change was much smaller than for the 16 h digested BP. Similarly, fluorescence lifetime was affected by the solvent polarity. With increasing solvent polarity, Channel 1 and Channel 2 fluorescence lifetime of both digested and native BP decreased. Note that the intensity ratios of native BP in PBS are closer to those of digested BP in ethanol, while the lifetimes of native BP in PBS are close to those of digested BP in PBS, which indicates that the lifetime is more sensitive to the solvent effect than intensity ratio.

Figure 8a shows a widefield image of a BP section, where two 4 mm diameter circular regions were digested with collagenase. As shown in the image, the degradation resulted in increased transparency of the digested regions. Figure 8b illustrates the method of preparing the samples, as discussed in "Materials and Methods" section. Channel 1 (390/18 nm) intensity ratio progressively decreased with digestion exposure time, as seen in the intensity ratio map (Fig. 8c) and the corresponding quantification (Fig. 8d). However, fluorescence lifetime remained constant over 2 days collagenase degradation (Figs. 8e and 8f).

DISCUSSION

Collagen is a dominant structural protein in most ECM.⁹ Studies have shown that over 70% per DW of native BP is formed by collagen.³⁵ Following collagenase degradation, collagen is removed from BP matrix and the amount of extracted collagen was found related to the time that the matrix is exposed to collagenase, as shown in the results of collagen assay and histological images (Fig. 1). It is well known that collagen exhibits a fluorescence emission peak at 390 nm band upon UV excitation.^{7,23,38} The fluorescence emission of our native BP

samples was primarily detected in Channel 1(390/18 nm) with a low signal detected in Channel 2(435/40 nm). This suggests the possibility of using BP auto fluorescence to monitor the collagen loss during collagenase degradation. The observation, by a previous study,⁸ of a positive correlation between pericardium collagen content and elastic moduli motivated the use of a tensile testing in this study to measure the change in Young's Modulus and UTS as a function of collagenase digestion time. From Table 1, it was found that the removal of collagen led to a decrease of Young's Modulus and UTS. The strong correlation observed between collagen content, Young's Modulus and UTS to ms-FLIm measurement results, demonstrates the potential of the ms-FLIm system for non-destructive assessment of the biochemical and biomechanical properties of BP during degradation processes.

Lewis *et al.* suggested measuring endogeneous UV fluorescence intensity for probing the biomechanical properties of cartilage, however, it is known that the absolute intensity measurement is strongly dependent on the imaging configuration and prone to artefacts.¹⁴ Therefore, in our study, the relative intensity ratio between different fluorescence emission bands and fluorescence lifetime are considered as better biomarkers for characterizing changes in BP during degradation. Intensity ratio is a measure of fluorescence emission spectrum and therefore related to matrix biochemical composition. The statistical analysis indicates that the collagen content, Young's Modulus and UTS are significantly correlated with the Channel 1 (390/18 nm) and Channel 2 (435/40 nm) intensity ratios (Figs. 5 and 6). In terms of fluorescence lifetime, the decreases in Channel 1 and Channel 2 lifetime agreed with the results of previous studies.^{17,18} Compared with intensity ratio, the correlation of lifetime with the conventional measurement results is marginally weaker. However, the lifetime measurement modality still has value because there are situations where only the lifetime changes while the spectrum remains the same, as observed by Manning *et al.* in their cartilage degradation study.¹⁸

As shown above, collagenase degradation caused the emission spectrum to red shift and the lifetime to decrease. One possible explanation is that the collagenase degradation caused a change of relative amounts of different fluorophores, for example, the ratio of pentosidine to pyridinoline, both of which are known crosslinking elements present in collagen matrices, and will fluoresce upon UV excitation.¹⁴ However, the bacterial collagenase we used is known to be highly active for digesting collagen by directly attacking the triple helical regions.⁶ For BP, a biomaterial dominated by collagen,³⁵ the effect of collagenase degradation is more likely to be a removal of whole collagen fibrils rather than specific components. Therefore, it is not likely that the observed spectral and lifetime changes were due to the relative changes of different fluorophores. A plausible explanation was proposed by Manning *et al.* who postulated that the decrease of lifetime resulted from the microenvironment changes of collagen crosslink sites within the fibrils during collagenase degradation.¹⁸ In this paper, we expand on this hypothesis by investigating the impact of solvent polarity on fluorescence emission. We found a spectral red shift and a lifetime decrease when the sample was exposed to solvent with higher polarity (Figs. 7a-7d). Both of these changes due to the solvent effect have been previously well studied.^{11,27} For this study, consider some of the fluorophores in a collagen fiber (represented by stars in Fig. 7e) to be located closer to the surface while the rest are inside the fiber, isolated from the solvent.

Since all measurements were performed with the samples surrounded by PBS, the surface fluorophores were exposed to an aqueous high polar solvent, such as water, causing the emission spectrum to red shift and fluorescence lifetime to decrease.² After collagenase degradation, the shrinkage of collagen fibers caused by the removal of collagen, gave rise to an increase ratio between fluorophores exposed to solvent and fluorophores isolated from solvent, magnifying the spectral red shift and the decrease of fluorescence lifetime.

A non-destructive label-free method to quantify biochemical and biomechanical properties provides many advantages compared to conventional destructive measurements, including the opportunity to profile the distribution of collagen content and mechanical properties of a heterogenous matrix and to visualize matrix defects. To demonstrate this, we artificially introduced localized defects to a BP matrix by digesting small areas (Fig. 8a). The sample preparation was described in section “Materials and Methods” and illustrated in Fig. 8b. The digested circular regions were easily distinguished in the intensity ratio map in Channel 1 (390/18 nm, Fig. 8c). As the digestion is limited by the small contact area between the collagenase and samples, we increased the maximum digestion exposure time to 2 days. A clear decreasing trend in Channel 1 intensity ratio with digestion exposure time (Fig. 8d) was consistent with the results of the BP degradation longitudinal study (Fig. 3a). However, the fluorescence lifetime remained the same after digestion, which contrasts with the decrease of lifetime observed in Fig. 4. This is likely attributed to the structural degradation caused by localized digestion is smaller than that in the former experiment where the whole sample is immersed in collagenase. The intensity ratio change (0.17, Fig. 8d) after 2 days digestion in the localized digestion configuration is even smaller than that after 16 h digestion in the former digestion experiment (0.25, Fig. 3a), corresponding to a lifetime change of 0.35 ns.

In conclusion, the collagen content, Young’s Modulus and UTS of native bovine pericardium have been shown to strongly correlate with the relative intensity ratio between different fluorescence emission bands, and significantly correlate with fluorescence lifetime. Thus, ms-FLIm is capable of non-destructively monitoring biochemical and biomechanical changes of BP during collagenase degradation. A model for predicting collagen content and the biomaterial’s mechanical properties using ms-FLIm metrics, such as intensity ratio and fluorescence lifetime, would be of great value for the tissue engineering community, as it could potentially replace conventional approaches by non-destructive, less costly, and faster measurements, enabling *in situ* monitoring of engineered biomaterials for regenerative medicine applications.

Supplementary Material

Refer to Web version on PubMed Central for supplementary material.

ACKNOWLEDGMENTS

This work is supported by the National Institutes of Health Grant.1R01 HL121068. We are grateful to Dr. Alyssa Panitch for providing the rheometer used in this study.

REFERENCES

1. Aguiari P, Fiorese M, Iop L, Gerosa G, and Bagno A. Mechanical testing of pericardium for manufacturing prosthetic heart valves. *Interact. Cardiovasc. Thorac. Surg* 22:72–84, 2016. [PubMed: 26489665]
2. Bell JE *Spectroscopy in Biochemistry*. Boca Ration: CRC Press, 1981.
3. Claramunt R, Alvarez-Ayuso L, Garcia-Paez JM, Ros A, and Casado MC. Changes in the mechanical properties of chemically treated bovine pericardium after a short uniaxial cyclic test. *Artif. Organs* 37:183–188, 2013. [PubMed: 23043423]
4. Croce AC, and Bottiroli G. Autofluorescence spectroscopy and imaging: a tool for biomedical research and diagnosis. *Eur. J. Histochem* 58:320–337, 2014.
5. Duan XJWH, Xu JP, Li L, Xu HY, and Wang QZ. Surgical pathology analysis of the causes of failure of 48 bioprosthetic heart valves in 40 Chinese cases. *Zhonghua Wai Ke Za Zhi* 54:6, 2016. [PubMed: 26792345]
6. Duarte AS, Correia A, and Esteves AC. Bacterial collagenases—a review. *Crit. Rev. Microbiol* 42:106–126, 2016. [PubMed: 24754251]
7. Elson DS, Jo JA, and Marcu L. Miniaturized sideviewing imaging probe for fluorescence lifetime imaging (FLIM): validation with fluorescence dyes, tissue structural proteins and tissue specimens. *New J. Phys* 9:127, 2007.
8. Filova E, Burdikova Z, Stankova L, Hadraba D, Svindrych Z, Schornik D, Bacakova L, Chlup H, Gultova E, Vesely J, Horny L and Zitny R. Collagen structures in pericardium and aortic heart valves and their significance for tissue engineering. In: 2013 E-Health and Bioengineering Conference (Ehb), 2013.
9. Gelse K Collagens—structure, function, and biosynthesis. *Adv. Drug Deliv. Rev* 55:1531–1546, 2003. [PubMed: 14623400]
10. Goncalves AC, Griffiths LG, Anthony RV, and Orton EC. Decellularization of bovine pericardium for tissueengineering by targeted removal of xenoantigens. *J. Heart Valve Dis* 14:212–217, 2005. [PubMed: 15792182]
11. Jones G, Jackson WR, Choi C, and Bergmark WR. Solvent effects on emission yield and lifetime for coumarin laser-dyes—requirements for a rotatory decay mechanism. *J. Phys. Chem* 89:294–300, 1985.
12. Jorge-Herrero E, Fernandez P, Turnay J, Olmo N, Calero P, Garcia R, Freile I, and Castillo-Olivares JL. Influence of different chemical cross-linking treatments on the properties of bovine pericardium and collagen. *Biomaterials* 20:539–545, 1999. [PubMed: 10213357]
13. Khanna RK, and Mokhtar E. Bovine pericardium in treating large corneal perforation secondary to alkali injury: a case report. *Indian J. Ophthalmol* 56:429–430, 2008. [PubMed: 18711278]
14. Lewis W, Padilla-Martinez JP, Ortega-Martinez A, and Franco W. Changes in endogenous UV fluorescence and biomechanical stiffness of bovine articular cartilage after collagenase digestion are strongly correlated. *J. Biophotonics* 10:1018, 2016. [PubMed: 27714971]
15. Li X, Guo Y, Ziegler KR, Model LS, Eghbalieh SD, Brenes RA, Kim ST, Shu C, and Dardik A. Current usage and future directions for the bovine pericardial patch. *Ann. Vasc. Surg* 25:561–568, 2011. [PubMed: 21276709]
16. Liu J, Sun Y, Qi J, and Marcu L. A novel method for fast and robust estimation of fluorescence decay dynamics using constrained least-squares deconvolution with Laguerre expansion. *Phys. Med. Biol* 57:843–865, 2012. [PubMed: 22290334]
17. Lutz V, Sattler M, Gallinat S, Wenck H, Poertner R, and Fischer F. Impact of collagen crosslinking on the second harmonic generation signal and the fluorescence lifetime of collagen autofluorescence. *Skin Res. Technol* 18:168–179, 2012. [PubMed: 21564311]
18. Manning HB, Nickdel MB, Yamamoto K, Lagarto JL, Kelly DJ, Talbot CB, Kennedy G, Dudhia J, Lever J, Dunsby C, French P, and Itoh Y. Detection of cartilage matrix degradation by autofluorescence lifetime. *Matrix Biol.* 32:32–38, 2013. [PubMed: 23266527]
19. Marcu L Fluorescence lifetime in cardiovascular diagnostics. *J. Biomed. Opt* 15:011106, 2010. [PubMed: 20210432]

20. Marcu L Fluorescence lifetime techniques in medical applications. *Ann. Biomed. Eng* 40:304–331, 2012. [PubMed: 22273730]
21. Muto A, Nishibe T, Dardik H, and Dardik A. Patches for carotid artery endarterectomy: current materials and prospects. *J. Vasc. Surg* 50:206–213, 2009. [PubMed: 19563972]
22. Nadkarni SK, Pierce MC, Park BH, de Boer JF, Whittaker P, Bouma BE, Bressner JE, Halpern E, Houser SL, and Tearney GJ. Measurement of collagen and smooth muscle cell content in atherosclerotic plaques using polarization-sensitive optical coherence tomography. *J. Am. Coll. Cardiol* 49:1474–1481, 2007. [PubMed: 17397678]
23. Phipps JE, Sun Y, Fishbein MC, and Marcu L. A fluorescence lifetime imaging classification method to investigate the collagen to lipid ratio in fibrous caps of atherosclerotic plaque. *Lasers Surg. Med* 44:564–571, 2012. [PubMed: 22886522]
24. Provencher S, and Deslauriers J. Late complication of bovine pericardium patches used for lung volume reduction surgery. *Eur. J. Cardiothorac. Surg* 23:1059–1061, 2003. [PubMed: 12829092]
25. Quinn KP, Sullivan KE, Liu Z, Ballard Z, Siokatas C, Georgakoudi I, and Black LD. Optical metrics of the extracellular matrix predict compositional and mechanical changes after myocardial infarction. *Sci. Rep* 6:35823, 2016. [PubMed: 27819334]
26. Schindelin J, Rueden CT, Hiner MC, and Eliceiri KW. The ImageJ ecosystem: an open platform for biomedical image analysis. *Mol. Reprod. Dev* 82:518–529, 2015. [PubMed: 26153368]
27. Sharma A, and Schulman SG. *Introduction to Fluorescence Spectroscopy*. New York: Wiley, 1999.
28. Simionescu DT, Lovekamp JJ, and Vyavahare NR. Degeneration of bioprosthetic heart valve cusp and wall tissues is initiated during tissue preparation: an ultrastructural study. *J. Heart Valve Dis* 12:226–234, 2003. [PubMed: 12701796]
29. Spoerl E, Wollensak G, and Seiler T. Increased resistance of crosslinked cornea against enzymatic digestion. *Curr. Eye Res* 29:35–40, 2004. [PubMed: 15370365]
30. Sun CR, Standish B, and Yang VXD. Optical coherence elastography: current status and future applications. *J. Biomed. Opt* 16:043001, 2011. [PubMed: 21529067]
31. Turunen MJ, Khayyeri H, Guizar-Sicairos M, and Isaksson H. Effects of tissue fixation and dehydration on tendon collagen nanostructure. *J. Struct. Biol* 199:209–215, 2017. [PubMed: 28760694]
32. Us MH, Sungun M, Sanioglu S, Pocan S, Cebeci BS, Ogus T, Ucak A, and Guler A. A retrospective comparison of bovine pericardium and polytetrafluoroethylene patch for closure of ventricular septal defects. *J. Int. Med. Res* 32:218–221, 2004. [PubMed: 15080027]
33. Wang YXY, and Li JS. Cholangioplasty by using a patch of bovine pericardium in treatment of stricture of extrahepatic bile duct. *Zhonghua Wai Ke Za Zhi* 32:269–270, 1994. [PubMed: 7842939]
34. Wong ML, Wong JL, Athanasiou KA, and Griffiths LG. Stepwise solubilization-based antigen removal for xenogeneic scaffold generation in tissue engineering. *Acta Biomater.* 9:6492–6501, 2013. [PubMed: 23321301]
35. Wong ML, Wong JL, Horn RM, Sannajust KC, Rice DA, and Griffiths LG. Effect of urea and thiourea on generation of xenogeneic extracellular matrix scaffolds for tissue engineering. *Tissue Eng. Part C* 22:700–707, 2016.
36. Yankelevich DR, Ma D, Liu J, Sun Y, Sun Y, Bec J, Elson DS, and Marcu L. Design and evaluation of a device for fast multispectral time-resolved fluorescence spectroscopy and imaging. *Rev. Sci. Instrum* 85:034303, 2014. [PubMed: 24689603]
37. Yao ES, Zhang H, Chen Y-Y, Lee B, Chew K, Moore D, and Park C. Increased $\beta 1$ Integrin is associated with decreased survival in invasive breast cancer. *Can. Res* 67:659, 2007.
38. Yova D, Hovhannisyann V, and Theodossiou T. Photo-chemical effects and hypericin photosensitized processes in collagen. *J. Biomed. Opt* 6:52–57, 2001. [PubMed: 11178580]

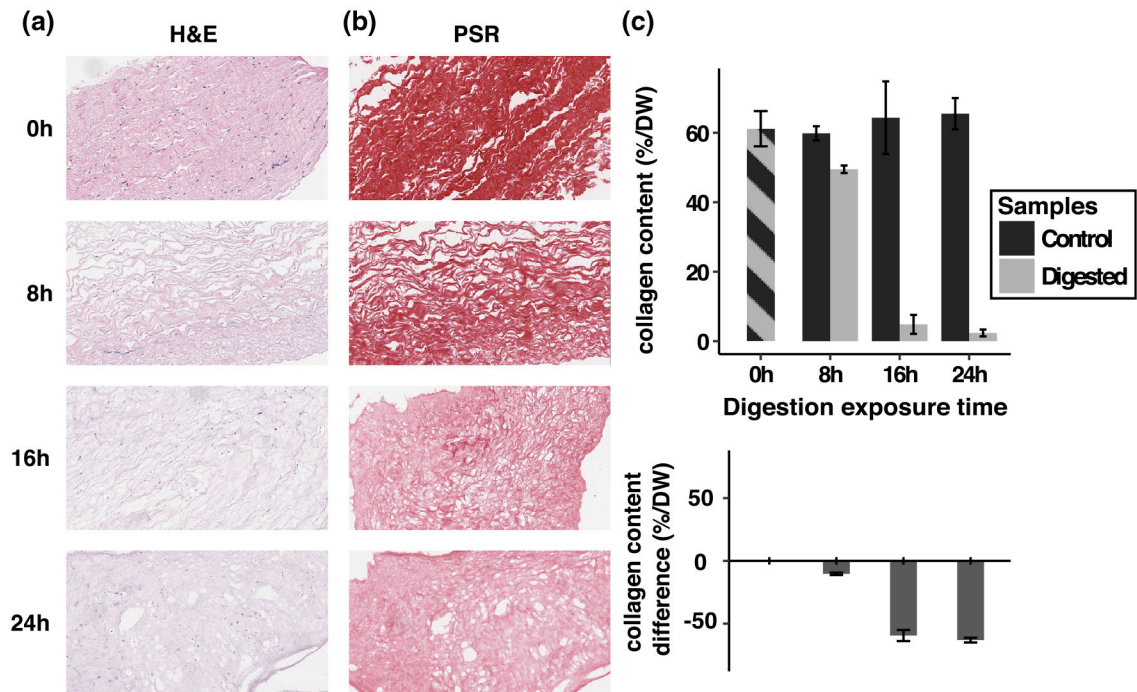


FIGURE 1.

Histology and collagen content measurements over different digestion exposure times. (a) Hematoxylin and eosin staining (H&E) and (b) Picro sirius red staining (PSR) of digested group at 0, 8, 16, 24 h time points; (c) Collagen content measured with hydroxyproline assay (above) and the unstandardized difference between the control group and digested group (below) over different digestion exposure time. Hatch pattern represents that the digested group and control group are from same samples.

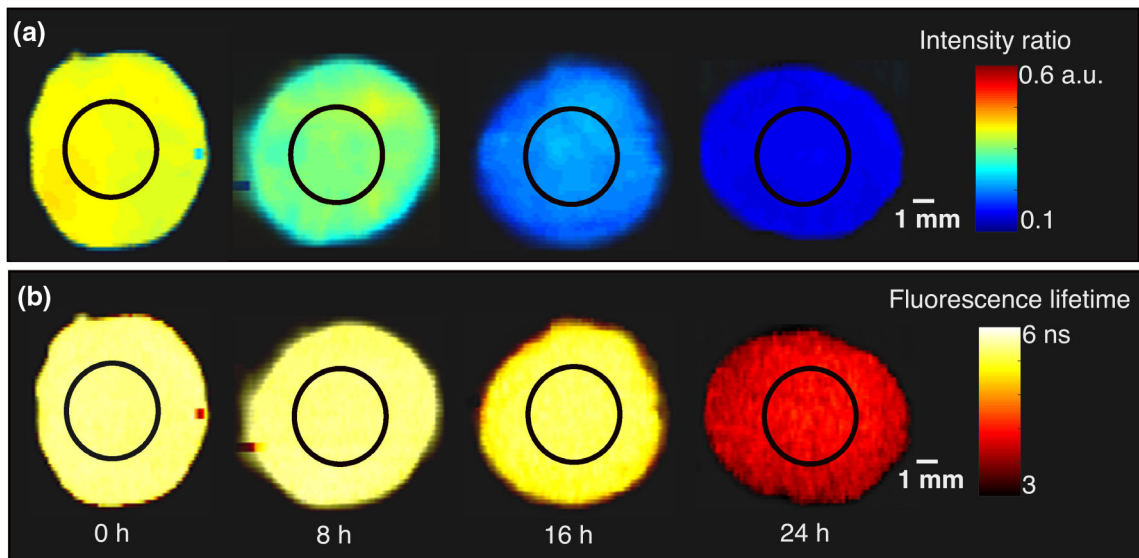


FIGURE 2.

FLIm maps of digested BP. (a) Intensity ratio and (b) fluorescence lifetime maps of the digested group at 0, 8, 16, and 24 h time points. The black circle represent the region of interest within which data were analyzed.

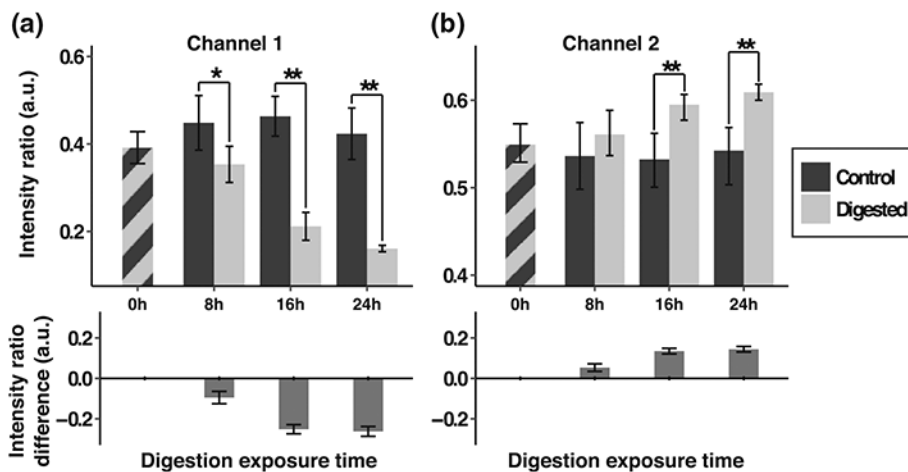


FIGURE 3.

Changes of intensity ratio over different digestion exposure times. Columns represent two channels: (a) Channel 1 (390/18 nm) and (b) Channel 2 (435/40 nm). The figures in the above row show the intensity ratio change over different digestion exposure time in both channels. The figures in the bottom row show the unstandardized mean difference between the control group and digested group over different digestion exposure time in both channels. Hatch pattern represents that the digested group and control group are from same samples (* $p < 0.05$; ** $p < 0.01$).

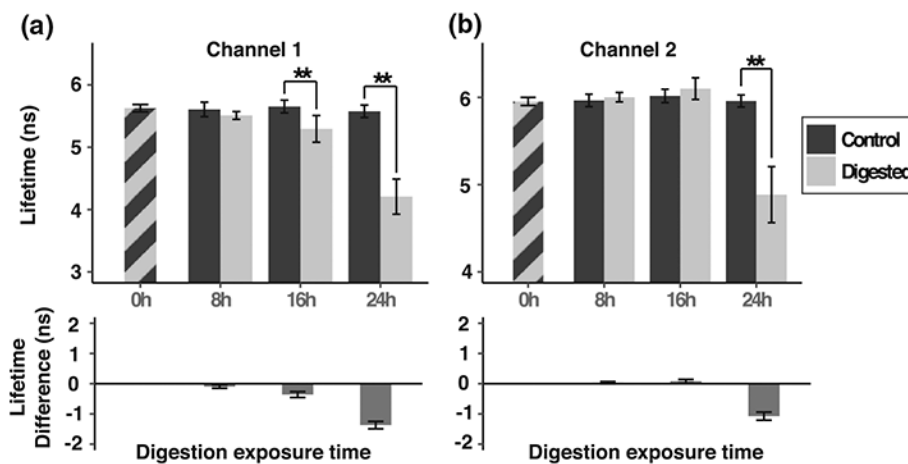


FIGURE 4.

Changes of fluorescence lifetime over different digestion exposure times. Columns represent two channels: (a) Channel 1 (390/18 nm) and (b) Channel 2 (435/40 nm). The figures in the above row show the fluorescence lifetime change over different digestion exposure time in both channels. The figures in the bottom row show the unstandardized mean difference between the control group and digested group over different digestion exposure time in both channels. Hatch pattern represents that the digested group and control group are from same samples (** $p < 0.01$).

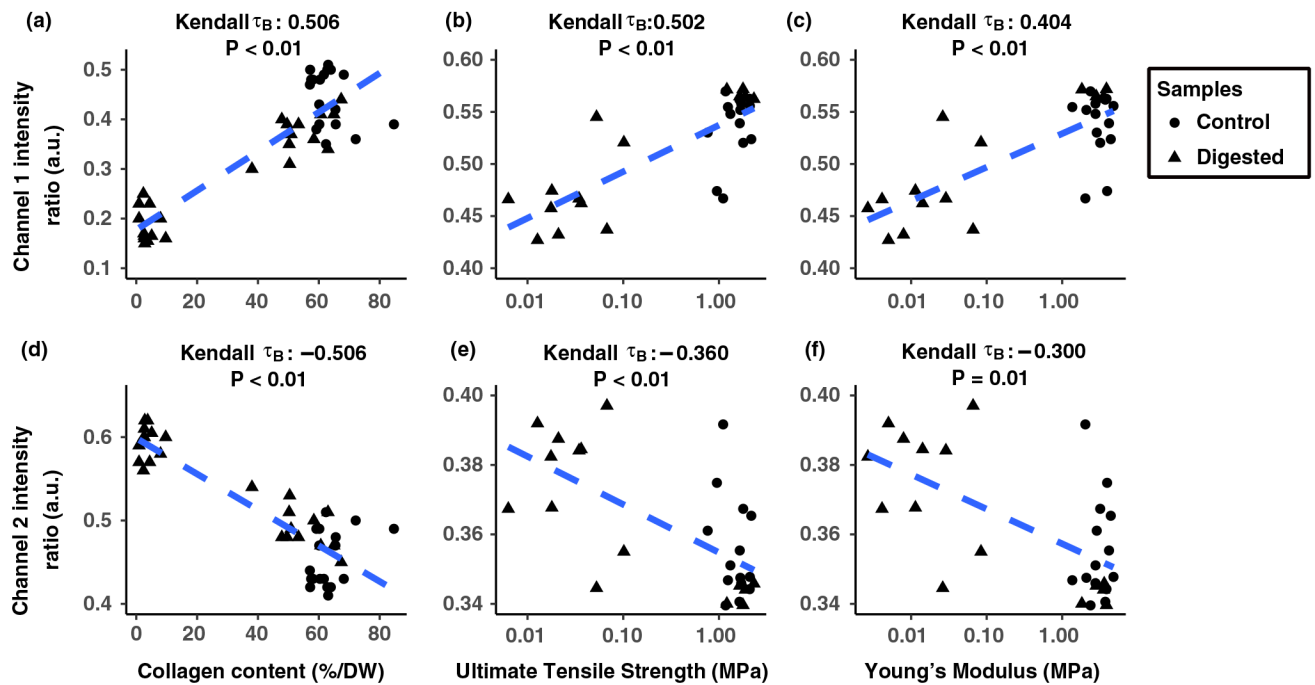
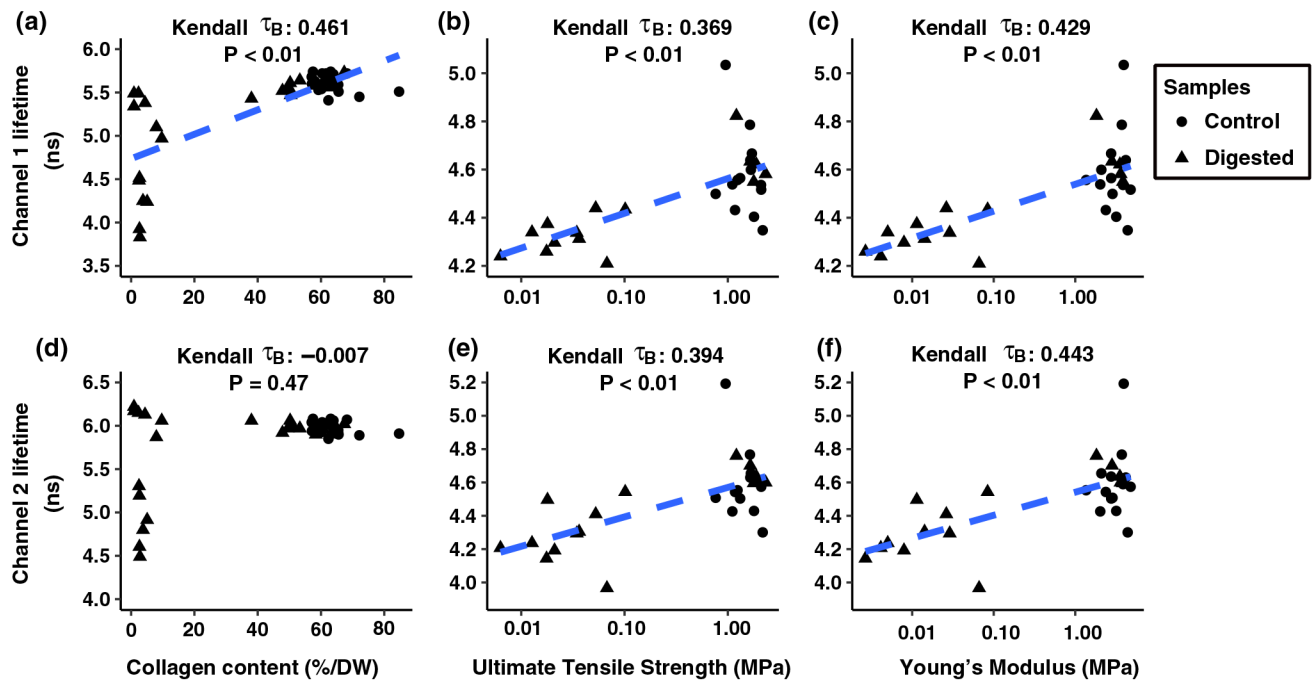


FIGURE 5.

Correlations of (a) Collagen content vs. Channel 1 (390/18 nm) intensity ratio, (b) Ultimate Tensile Strength (UTS) vs. Channel 1 intensity ratio, (c) Young's Modulus vs. Channel 1 intensity ratio and (d) Collagen content vs. Channel 2 (435/40 nm) intensity ratio, (e) UTS vs. Channel 2 intensity ratio, (f) Young's Modulus vs. Channel 2 intensity ratio. The Kendall τ_B and p value of each combination are shown in the plot. The trend were demonstrated by the blue dashed line for the variables that are significant correlated ($p < 0.01$)

**FIGURE 6.**

Correlations of (a) Collagen content vs. Channel 1 (390/18 nm) lifetime, (b) Ultimate Tensile Strength (UTS) vs. Channel 1 lifetime, (c) Young's Modulus vs. Channel 1 lifetime and (d) Collagen content vs. Channel 2 (435/40 nm) lifetime, (e) UTS vs. Channel 2 lifetime, (f) Young's Modulus vs. Channel 2 lifetime. The Kendall τ_B and p value of each combination are shown in the plot. The trend were demonstrated by the blue dashed line for the variables that are significant correlated ($p < 0.01$).

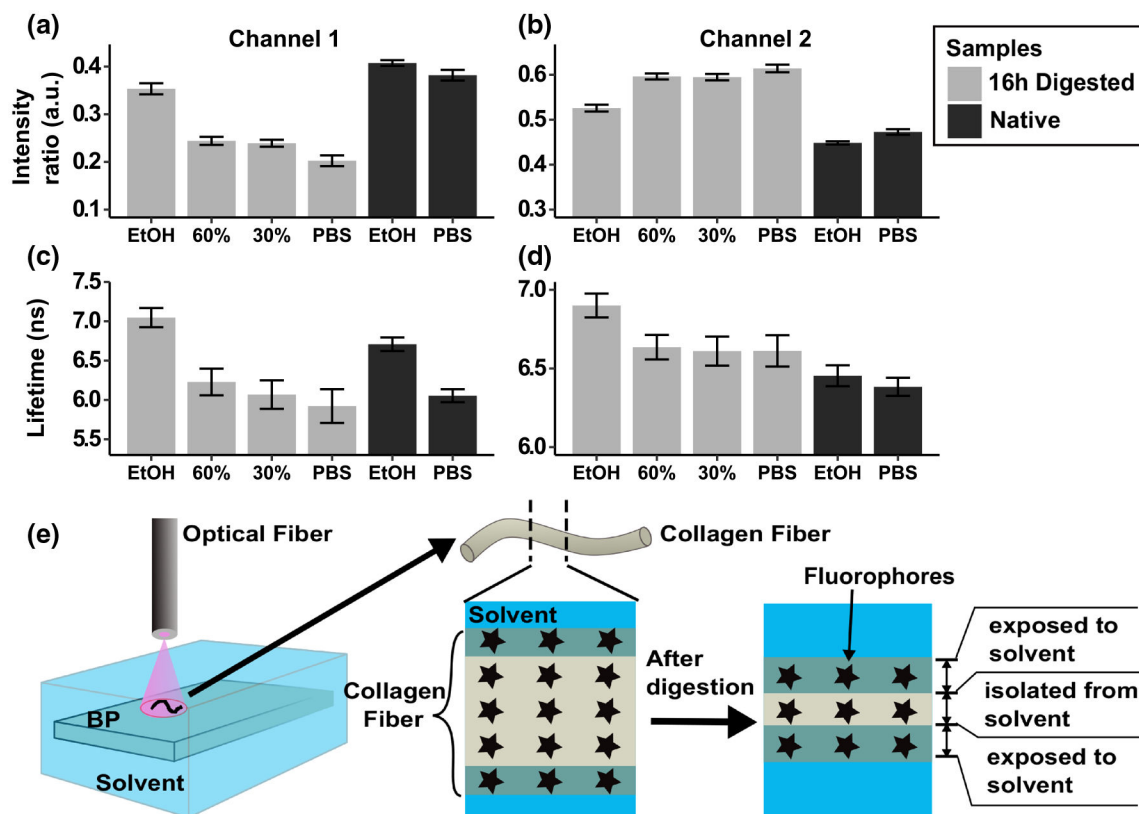
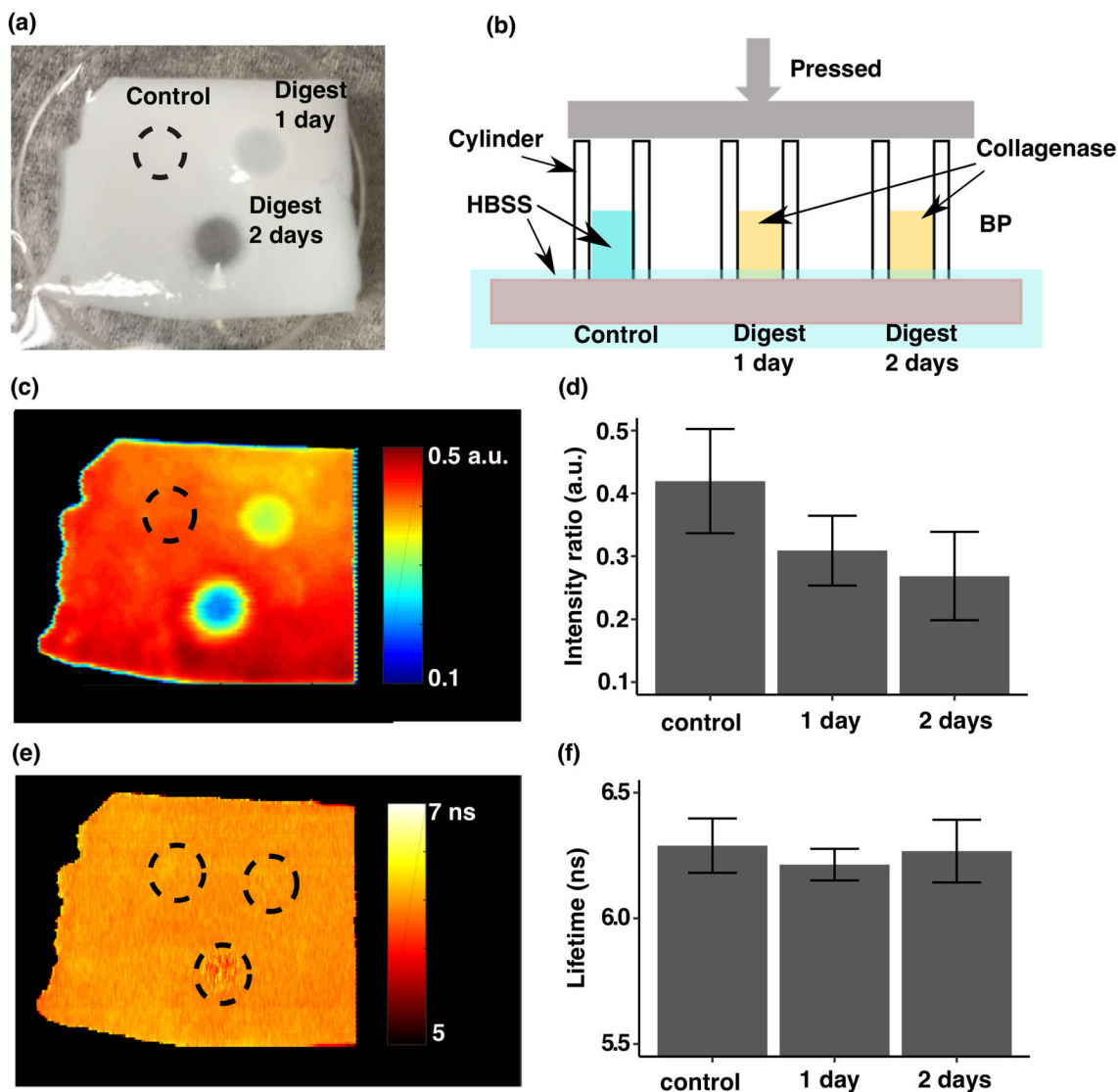


FIGURE 7.

Lifetime and intensity ratio changes due to the solvent Effect. (a) Channel 1 (390/18 nm) and (b) Channel 2 (435/40 nm) intensity ratio of the native BP and 16 h digested BP in different solvents; (c) Channel 1 and (d) Channel 2 lifetime of the native BP and 16 h digested BP in different solvents. EtOH represents pure ethanol, X% represent X% of solution is ethanol. PBS represents pure PBS solution. (e) Schematic of the solvent effect hypothesis for explaining the change observed on fluorescence spectra and lifetime. The measured BP fluorescence signal has two main contributions: (1) fluorophores on the surface whose signal is affected by the surrounding solvent; (2) fluorophores isolated from the solvent whose signal will not be affected by it. After collagenase degradation, the structural changes on the collagen fibers result in relatively more fluorophores get exposed to solvent and are affected by the solvent effect.

**FIGURE 8.**

Localized digestion on BP. (a) Widefield image of the localized digested BP. The black dashed circle represents the control area. The less transparent area is processed by 1 day digestion and the most transparent area is processed by 2 days digestion; (b) Schematic of the localized digestion setup: three cylinders containing corresponding treatment solutions (HBSS as control, 200 U ml⁻¹ of collagenase for 1 day, and for 2 days as digested groups) were pressed against the tissue to avoid solution leaking out from the bottom. The cylinders were removed and sample was rinsed in PBS prior to imaging; (c) Channel 1 (390/18 nm) intensity ratio map of a localized digested BP and (d) average Channel 1 intensity ratios of control, 1 day digested and 2 days digested areas; (e) Channel 1 fluorescence lifetime map of a localized digested BP. The red dashed circles showed the control and digested regions (f) average Channel 1 fluorescence lifetime of control, 1 day digested and 2 days digested areas. The barplots of intensity ratio and lifetime were based on the average results of three individual localized digested experiments.

TABLE 1.

Young's modulus and UTS of the control and digested groups at 0, 8 and 12 h time points.

Digestion exposure time (h)	Young's modulus (MPa)		UTS (MPa)	
	Control	Digested	Control	Digested
0	3.09 ± 1.52	3.13 ± 0.82	1.65 ± 0.52	1.77 ± 0.40
8	3.00 ± 1.04	0.03 ± 0.03	1.66 ± 0.38	0.05 ± 0.03
12	3.38 ± 0.63	0.02 ± 0.03	1.29 ± 0.44	0.03 ± 0.02